Journal of Materials Science & Technology ■■ (2016) ■■–■■

Contents lists available at ScienceDirect

Journal of Materials Science & Technology

journal homepage: www.jmst.org

Comparative Study on the Corrosion Resistance of Al–Cr–Fe Alloy Containing Quasicrystals and Pure Al

R.T. Li [1], Vinod K. Murugan [2], Z.L. Dong [2,*], K.A. Khor [1,*]

[1] *School of Mechanical and Aerospace Engineering, Nanyang Technological University, 50 Nanyang Avenue, Singapore 639798, Singapore*
[2] *School of Materials Science and Engineering, Nanyang Technological University, 50 Nanyang Avenue, Singapore 639798, Singapore*

ARTICLE INFO

Article history:
Received 10 April 2016
Received in revised form
3 June 2016
Accepted 27 June 2016
Available online

Key words:
Quasicrystal
Spark plasma sintering
Microstructure
Corrosion resistance

Al–Cr–Fe alloy containing quasicrystals has been consolidated using spark plasma sintering (SPS). Its corrosion resistance properties were comparatively investigated with pure Al by electrochemical methods in 3.5 wt% NaCl solution. Their corrosion current density was also compared with that of three commercial steels—316 stainless steel, AISI 440C stainless steel and AISI H13 tool steel. Al–Cr–Fe alloy exhibits nobler corrosion potential and evident passivation with a potential range of around 150 mV while no passivation of pure Al sample is seen. The corrosion resistance of Al–Cr–Fe alloy is less than that of pure Al, but is close to that of 316 stainless steel and superior to that of AISI 440C stainless steel and AISI H13 tool steel.

1. Introduction

Owing to their special atomic arrangement (with rotational symmetries but without translational symmetries), quasicrystals (QCs) exhibit unique properties, including low surface energy, low thermal conduction, high hardness, low friction, and good oxidation resistance[1–5]. As a consequence of these attractive properties, QCs have various potential applications in catalysis[6,7], hydrogen storage[8], reinforcement of composites[9–12], and coatings[13,14]. Al–Cr–Fe QCs are expected to exhibit excellent corrosion resistance due to the high Al and Cr contents. However, they are relatively less studied than other Al-based QCs like Al–Cu–Fe, especially in the aspect of corrosion resistance properties. To the best of our knowledge, no report on the corrosion properties of Al–Cr–Fe alloy is available in the literature. Therefore, there is a need to study corrosion resistance properties of Al–Cr–Fe QCs.

QCs generally exist in a small compositional range. Accordingly, in the Al–Cr–Fe alloys of practical importance, QCs typically coexist with crystalline phases, which have very close composition and local atomic arrangement to them. These crystalline phases are often called approximants. This means that not only QCs but also their approximants influence the corrosion behavior of the alloy in practical applications. Therefore, it is of great importance to investigate the corrosion behavior of Al–Cr–Fe alloy containing both QCs and their approximants. As the alloy contains around 70 at.% of Al, a comparative study of the corrosion behavior of Al–Cr–Fe alloy and pure Al makes the corrosion resistance properties of Al–Cr–Fe more comprehensible. In addition, as good candidates for coatings, QCs possess as high hardness as the hardest commercial steels[15]. Thus, the corrosion resistance of Al–Cr–Fe alloy was also compared with that of three commercial steels—316 stainless steel, AISI 440C stainless steel and AISI H13 tool steel.

Al–Cr–Fe powders have been commercially produced using gas atomization[16]. In order to facilitate the test of corrosion resistance, these powders need to be consolidated into bulk materials. Spark plasma sintering (SPS) was employed as the consolidation technique in this report. In the SPS process, several mechanisms promote sintering: joule heat generates a rapid local temperature increase; external pressure promotes particle rearrangement; spark plasma activates the particle surface and promote the material transfer[17–20]. As a result of its unique sintering mechanisms, SPS can consolidate metals and ceramic very rapidly at a relatively low temperature. It is worth mentioning that SPS has also been used to consolidate QCs[21].

In the present work, we prepared Al–Cr–Fe bulk alloys using SPS. Its corrosion resistance properties were comparatively studied with commercially pure Al and also compared with three commercial steels–316 stainless steel, AISI 440C stainless steel and AISI H13 tool steel.

---

* Corresponding authors. Fax: +65 6791 2397;
E-mail addresses: ZLDONG@ntu.edu.sg (Z.L. Dong); MKAKHOR@ntu.edu.sg (K.A. Khor).

http://dx.doi.org/10.1016/j.jmst.2016.07.005

Please cite this article in press as: R.T. Li, Vinod K. Murugan, Z.L. Dong, K.A. Khor, Comparative Study on the Corrosion Resistance of Al–Cr–Fe Alloy Containing Quasicrystals and Pure Al, Journal of Materials Science & Technology (2016), doi: 10.1016/j.jmst.2016.07.005

Table 1
Composition of commercially pure Al pellet

Element	Si	Fe	Total impurity	Al
Content	<0.015	<0.015	<0.03	>99.97

2. Experimental

2.1. Sample preparation

The $Al_{70}Cr_{20}Fe_{10}$ powders were purchased from Saint Gobian, France. They were prepared by gas atomization and consolidated in SPS system (Sumitomo Coal Mining Company, Ltd., Tokyo, Japan). $Al_{70}Cr_{20}Fe_{10}$ powders with weight of 1 g was loaded into a graphite die with an inner diameter of 10 mm and pressed by two graphite punches. A thermocouple inserted into the blind hole at the external wall of the graphite die was used to measure temperature. The consolidation was conducted at 800 °C for 30 min with a constant heating/cooling rate of 100 °C/min under a uniaxial pressure of 50 MPa in vacuum (<10 Pa). A pellet (Φ10 mm × 2 mm) was cut from a commercially pure Al bar (Titan, Singapore) as the pure Al sample for the corrosion resistance tests. The composition of the pure Al pellet is shown in Table 1. Obviously, the contents of Si, Cu and Fe are very low.

2.2. Microstructural characterization of the sintered alloy

X-ray diffraction (XRD) analysis (using a PANalytical Empyrean X-ray diffractometer, CuK_α radiation) was performed to determine the phases of Al–Cr–Fe pellets. Scanning electron microscopy (SEM, JEOL JSM-5600LV), energy-dispersive spectroscopy (EDS, Oxford), and transmission electron microscopy (JEOL 2100F) were employed for the characterization of the microstructure.

2.3. Electrochemical measurements

For comparison, both pure Al pellet and Al–Cr–Fe were tested. The samples were first grinded with 600-grit SiC paper and then with 3-µm diamond suspension. All electrochemical analyses including open circuit potential (OCP) measurement, potentiodynamic polarization (PDP) scans and electrochemical impedance spectroscopy (EIS) were conducted using a 600TM Potentiostat/Galvanostat/ZRA (Gamry Instruments, Inc., Warminster, PA, USA) potentiostat. The obtained data were analyzed using Gamry Echem Analyst (version 5.58) software.

A three-electrode system was used with the pure Al or Al–Cr–Fe pellet as the working electrode, Pt as the counter electrode and a silver/silver chloride (i.e. Ag|AgCl, 0.210 V vs. standard hydrogen electrode) electrode as the reference electrode. EIS tests were conducted at an OCP with 10 mV perturbation and ten points per decade. The frequency range was from 100 kHz to 10 mHz. These tests were performed after the corrosion potential become stabilized with time, in 3.5 wt% NaCl solution at a room temperature of 25 °C. The experimental results were interpreted based on an equivalent electrical circuit by using a suitable fitting.

Following EIS, polarization measurements were conducted after a delay of ten seconds. The polarization measurements were taken from a potential of –300 mV_{SCE} (cathodic) relative to the OCP and was stopped at an anodic potential where the anodic current increased dramatically, at a scan rate of 1 mV/s. The linear extrapolation of Tafel region of the polarization curves was adopted to obtain the corrosion potential (E_{corr}) and corrosion current (I_{corr}).

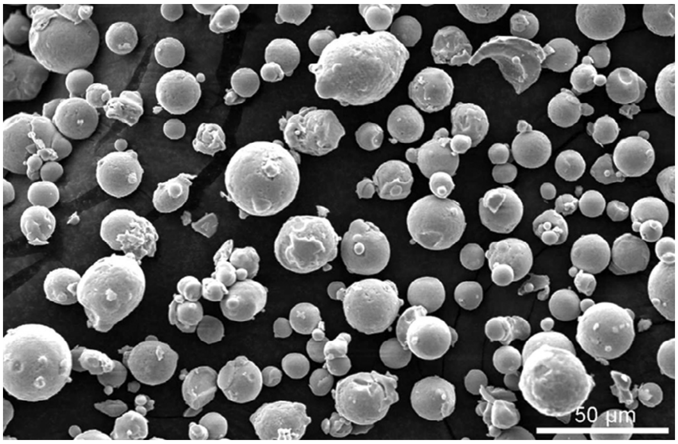

Fig. 1. Morphology of as-received Al–Cr–Fe powders.

3. Results and Discussion

3.1. Phases and microstructure

Fig. 1 shows the morphology of as-received Al–Cr–Fe powders. These particles exhibit typical morphology of gas-atomized powders: the surfaces of small particles are very smooth, while large particles present rougher surfaces and often have satellite particles. The spherical particles have a size ranging from several microns to around 30 µm.

The microstructure of the sintered Al–Cr–Fe pellets is exhibited in Fig. 2. The SEM backscattered electron (BSE) image (Fig. 2(a)) shows that dense pellets have been obtained with inter-particle boundaries hardly visible. In the image there are two types of regions—bright and gray. The bright regions are dispersed in the image, as indicated by the arrows. As phases with larger atomic number produce more backscattered electrons and are correspondingly brighter in the BSE image, it can be concluded that these bright regions have a larger average atomic number, i.e., the atomic percent of Cr and/or Fe is higher in these regions than in gray ones. EDX analysis further reveals that the Cr content is higher in these bright regions than that in the gray regions while the opposite is true for Al and Fe: the composition of the bright regions is around $Al_{66.3\pm0.8}Cr_{24.4\pm0.5}Fe_{9.3\pm0.2}$ and that of the grey regions is around $Al_{70.2\pm0.9}Cr_{18.6\pm0.4}Fe_{11.2\pm0.3}$. Fig. 2(b) is the scanning transmission electron microscope (STEM) image. From this image, it can be seen that most grains are polygonal and their size is in sub-micrometer to micrometer scale. As the size of bright regions in Fig. 2(a) is generally larger than that of grains in Fig. 2(b), it can be inferred that the bright regions in Fig. 2(a) may consist of multiple grains. The phases present in the sintered Al–Cr–Fe pellets were reported in our previous report [21]–icosahedral phase (I-AlCrFe), decagonal phase (D-AlCrFe), $Al_8(Cr,Fe)_5$ and $Al_9(Cr,Fe)_4$. Their crystallographic and compositional information can also be found there. As the morphological and compositional differences between the two crystalline phases ($Al_8(Cr,Fe)_5$ and $Al_9(Cr,Fe)_4$) and between two quasicrystalline phases (I-AlCrFe and D-AlCrFe) are not evident, it is difficult to determine the distribution of these phases by direct observation or compositional mapping. However, it can be inferred that the content of crystals in the bright regions is higher than that in the gray regions because $Al_8(Cr,Fe)_5$ and $Al_9(Cr,Fe)_4$ have a larger average atomic number than I-AlCrFe and D-AlCrFe.

3.2. Corrosion resistance properties

OCP measurements, which provide some indication of the reactivity of the metal surface, were taken. The results are shown in

Please cite this article in press as: R.T. Li, Vinod K. Murugan, Z.L. Dong, K.A. Khor, Comparative Study on the Corrosion Resistance of Al–Cr–Fe Alloy Containing Quasicrystals and Pure Al, Journal of Materials Science & Technology (2016), doi: 10.1016/j.jmst.2016.07.005